Article

Stern–Gerlach Experiments of One-Dimensional Metal–Benzene Sandwich Clusters: M(CH) (M = Al, Sc, Ti, and V)

Ken Miyajima, Satoshi Yabushita, Mark B. Knickelbein, and Atsushi Nakajima

J. Am. Chem. Soc., **2007**, 129 (27), 8473-8480• DOI: 10.1021/ja070137q • Publication Date (Web): 19 June 2007

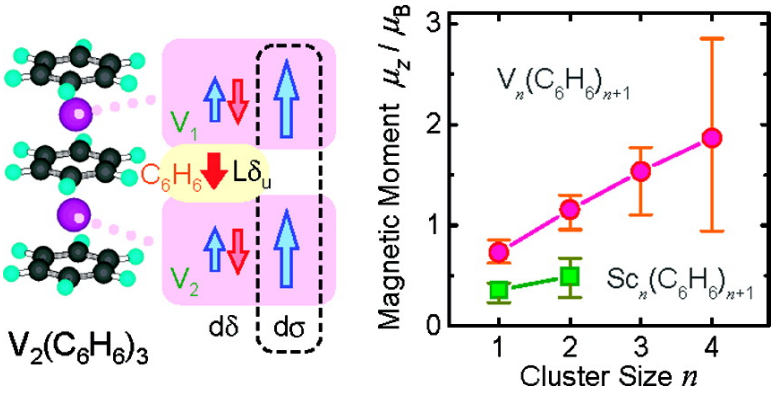

More About This Article

Additional resources and features associated with this article are available within the HTML version:

- Supporting Information
- Links to the 16 articles that cite this article, as of the time of this article download
- Access to high resolution figures
- Links to articles and content related to this article
- Copyright permission to reproduce figures and/or text from this article

View the Full Text HTML

J|A|C|S
ARTICLES
Published on Web 06/19/2007

Stern−Gerlach Experiments of One-Dimensional Metal−Benzene Sandwich Clusters: $M_n(C_6H_6)_m$ (M = Al, Sc, Ti, and V)

Ken Miyajima,[†] Satoshi Yabushita,[†] Mark B. Knickelbein,[‡] and Atsushi Nakajima*[,†,§]

Contribution from the Department of Chemistry, Faculty of Science and Technology, Keio University, 3-14-1 Hiyoshi, Kohoku-ku, Yokohama 223-8522, Japan, Chemistry Division and Center for Nanoscale Materials, Argonne National Laboratory, Argonne, Illinois 60439, and CREST, Japan Science and Technology Agency (JST), c/o Department of Chemistry, Keio University, Yokohama 223-8522, Japan

Received January 8, 2007; E-mail: nakajima@chem.keio.ac.jp

Abstract: A molecular beam of multilayer metal−benzene organometallic clusters $M_n(C_6H_6)_m$ (M = Al, Sc, Ti, and V) was produced by a laser vaporization synthesis method, and their magnetic deflections were measured. Multidecker sandwich clusters of transition-metal atoms and benzene $Sc_n(C_6H_6)_{n+1}$ (n = 1, 2) and $V_n(C_6H_6)_{n+1}$ (n = 1−4) possess magnetic moments that increase monotonously with n. The magnetic moments of $Al(C_6H_6)$, $Sc_n(C_6H_6)_{n+1}$, and $V_n(C_6H_6)_{n+1}$ are smaller than that of their spin-only values as a result of intracluster spin relaxation, an effect that depends on the orbital angular momenta and bonding characters of the orbitals containing electron spin. While $Ti(C_6H_6)_2$ was found to be nonmagnetic, $Ti_n(C_6H_6)_{n+1}$ (n = 2, 3) possess nonzero magnetic moments. The mechanism of ferromagnetic spin ordering in $M_2(C_6H_6)_3$ (M = Sc, Ti, V) is discussed qualitatively in terms of molecular orbital analysis. These sandwich species represent a new class of one-dimensional molecular magnets in which the transition-metal atoms are formally zerovalent.

1. Introduction

Magnetism in one-dimensional systems has been the subject of continuous theoretical and experimental research for decades. Progress in atomic/molecular engineering has made it possible to build one-dimensional (1D) metal chains on suitable substrates.[1] Many examples of single molecule magnets and magnetic molecular chains that can be classified as 0D and 1D magnets have been synthesized and characterized.[2−4] These new magnetic systems have drawn much attention for their potential applications in spin electronics.[5] Likewise, significant advances have been made on the synthesis of low-dimensional linear systems composed of stacked organometallic units.[6] Organometallic systems are promising precursors for the building of novel magnetic materials in which the presence of unpaired electron spins plays an important role in determining chemistry and physics.[7−9] Despite of difficulty of synthesizing such materials, the properties of some oligonuclear organometallic sandwich compounds have been studied. Paramagnetic metal-π complexes having sandwich structures have been the subject of a variety of fundamental physical studies.[10] Magnetic susceptibility studies of "tripledecker" sandwich complexes, for example, suggest that both the intermetallic separation and the chemical nature of the ligand bridge have a significant influence on their magnetism.[11]

In the past decade, it has been shown that organometallic complexes can be efficiently synthesized as polynuclear clusters in molecular beams via the gas-phase reaction of laser-vaporized metal atoms with benzene.[12,13] Subsequent spectroscopic studies and other characterization methods have confirmed that these species indeed possess multidecker sandwich structures.[12,14,15] Studies of organic ferromagnets indicate that the presence of a diamagnetic molecule between a pair of radicals in a stack can

[†] Keio University.
[‡] Argonne National Laboratory.
[§] CREST, Japan Science and Technology Agency (JST).

(1) Gambardella, P.; Dallmeyer, A.; Maiti, K.; Malagoll, M. C.; Eberhardt, W.; Kern, K.; Carbone, C. *Nature* **2002**, *416*, 301.
(2) Gatteschi, D.; Caneschi, A.; Pardi, L.; Sessoli, R. *Science* **1994**, *265*, 1054.
(3) Caneschi, A.; Gatteschi, D.; Lalioti, N.; Sangregorio, C.; Sessoli, R.; Venturi, G.; Vindigni, A.; Rettori, A.; Pini, M. G.; Novak, M. A. *Angew. Chem., Int. Ed.* **2001**, *40*, 1760.
(4) Clérac, R.; Miyasaka, H.; Yamashita, M.; Coulon, C. *J. Am. Chem. Soc.* **2002**, *124*, 12837.
(5) Naitabdi, A.; Bucher, J.-P.; Gerbier, P.; Rabu, P.; Drillon, M. *Adv. Matter.* **2005**, *17*, 1612.
(6) Rosenblum, M.; Nuget, H. M.; Jang, K.-S.; Labes, M. M.; Cahalane, W.; Klemarczyk, P.; Reiff, W. M. *Macromolecules* **1995**, *28*, 6330.
(7) Kollmar, C.; Kahn, O. *Acc. Chem. Res.* **1993**, *26*, 259−265.
(8) Miller, J. S.; Epstein, A. J. *Angew. Chem., Int. Ed. Engl.* **1994**, *88*, 385 and references therein.
(9) Yoshizawa, K.; Hoffmann, R. *J. Am. Chem. Soc.* **1995**, *117*, 6921.
(10) Hulliger, J. *Mol. Phys.* **1987**, *60*, 97.
(11) Beck, V.; Cowley, A. R.; O'Hare, D. *Organometallics* **2004**, *23*, 4265.
(12) (a) Hoshino, K.; Kurikawa, T.; Takeda, H.; Nakajima, A.; Kaya, K. *J. Phys. Chem.* **1995**, *99*, 3053. (b) Nakajima, A.; Kaya, K. *J. Phys. Chem. A* **2000**, *104*, 176. (c) Miyajima, K.; Muraoka, K.; Hashimoto, M.; Yasuike, T.; Yabushita, S.; Nakajima, A.; Kaya, K. *J. Phys. Chem. A* **2002**, *106*, 10777.
(13) Jena, P.; Castleman, A. W., Jr. *Proc. Natl. Acd. Sci. U.S.A.* **2006**, *103*, 10560.
(14) Weis, P.; Kemper, P. R.; Bowers, M. T. *J. Phys. Chem. A* **1997**, *101*, 8207.
(15) Rayane, D.; Allouche, A.-R.; Antoine, R.; Broyer, M.; Compagnon, I.; Dugourd, P. *Chem. Phys. Lett.* **2003**, *375*, 506.

10.1021/ja070137q CCC: $37.00

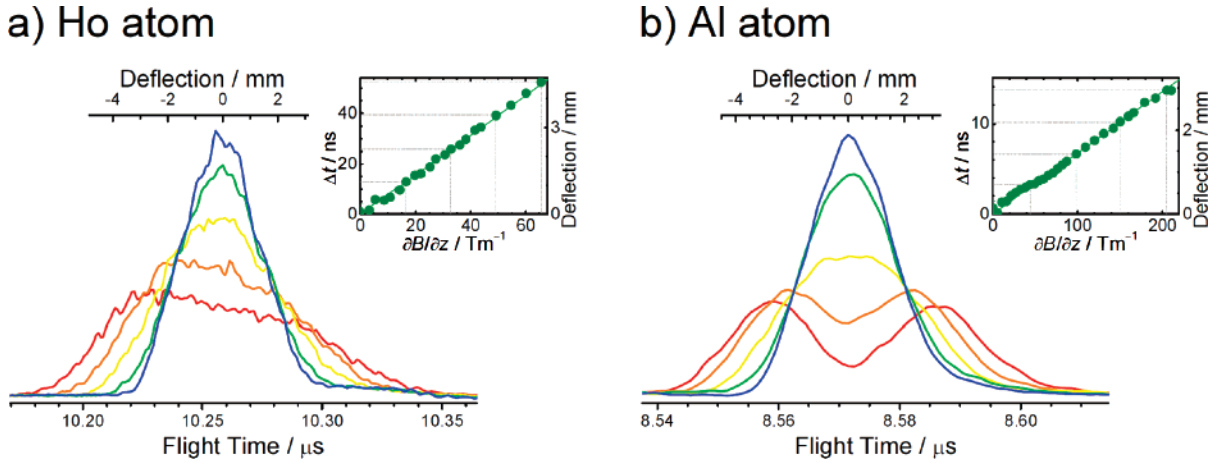

Figure 1. Position-sensitive TOF spectra of Ho atoms and Al atoms with various applied magnetic-field gradients. The sharpest peak (blue line) corresponds to the mass spectrum recorded without magnetic field for both cases. Inset plots show the magnetic deflection of the outmost beamlet in the magnetic-field gradient. In the plot, dots emphasized with dashed lines correspond to field broadened TOF spectra recorded at each magnetic-field gradient. Cluster source temperatures were 151 and 152 K for Ho and Al, respectively.

lead an effective ferromagnetic ordering among the radical spins.[16] This suggests that the sandwich structure is a suitable motif for producing ferromagnetic ordering of electron spins contained on metal atoms in organometallic clusters. Fortuitously, it is somewhat easier to achieve ferromagnetic spin alignment in such systems as compared to pure organic magnetic materials, for which a pronounced propensity exists toward antiferromagnetic interactions. Quantum chemical calculations have shown that the electronic structure of multilayered $M_n(C_6H_6)_{n+1}$ clusters (M = Ti, V, and Cr) is characterized by a delocalized electron density along the molecular axis originating from d_δ bonding orbitals and d_σ nonbonding orbitals localized on the metal valence orbital.[17] The overall magnetic moments of these multidecker clusters will depend on whether the d electrons have parallel or antiparallel spin coupling.

Here we present the results of magnetic deflection experiments obtained for metal−benzene clusters, $M_n(C_6H_6)_m$ (M = Al, Sc, Ti and V). Since the number of valence electrons in $Sc(C_6H_6)_2$, $Ti(C_6H_6)_2$, and $V(C_6H_6)_2$ complexes are 15, 16, and 17, respectively, an unpaired electron exists on the constituent Sc and V atoms, but not on the Ti atoms. It follows that the spin multiplicity of $M_n(C_6H_6)_m$ multidecker sandwich clusters is determined by the coupling of any unpaired electron spins on each metal atom. As reported in a previous Communication, the magnetic moments of $V_n(C_6H_6)_{n+1}$ sandwich clusters were found to increase with the number of vanadium atoms in the cluster, showing that the unpaired electrons on the metal atoms couple ferromagnetically.[18] In this paper, we present the results for systematic studies of the magnetic deflections of Sc−, Ti−, and V−C_6H_6 clusters. Molecular orbital considerations predict that $Sc_n(C_6H_6)_{n+1}$ clusters have one unpaired electron in each d_δ bonding orbital, and $V_n(C_6H_6)_{n+1}$ clusters have one unpaired electron in each d_σ orbital. By contrast $Ti(C_6H_6)_2$ is predicted to have no unpaired electrons. We have found that both $Sc_n(C_6H_6)_{n+1}$ and $V_n(C_6H_6)_{n+1}$ clusters exhibit deflections consistent with ferromagnetic spin alignment of the unpaired electrons. The magnitude of the deflections in these systems are somewhat attenuated because of intracluster spin relaxation, the extent of which depends on the orbital angular momenta and bonding characters of d_δ and d_σ orbitals. We will elucidate the mechanism of ferromagnetic spin ordering in $V_2(C_6H_6)_3$ in particular, and present qualitative analyses of the $Sc_2(C_6H_6)_3$ and $Ti_2(C_6H_6)_3$ deflection results using molecular orbital arguments.

2. Experimental Section

The magnetic moments of the $M_n(C_6H_6)_m$ complexes were determined by a Stern−Gerlach molecular-beam magnetic deflection experiment.[19] Details of the experimental setup have been previously described elsewhere.[18,19] Briefly, Sc, Ti, or V metal vapor produced via laser vaporization of the corresponding metal target was carried by helium into a flow tube reactor, where benzene vapor was injected. The subsequent reaction of the metal atoms and benzene forms a variety of $M_n(C_6H_6)_m$ product species. The ~4 ms residence time of the complexes within the flow reactor was sufficient to ensure that the complexes were thermally equilibrated to the flow tube temperature (variable between 60 and 300 K) prior to expansion into vacuum.[19] A collimated molecular beam containing the clusters is passed through the gap of a dipole gradient electromagnet with field gradients $\partial B/\partial z$ up to 210 Tm^{-1}. Downstream of the magnet, the clusters were photoionized by a spatially expanded ArF excimer laser (λ = 193 nm; $h\nu$ = 6.42 eV), with the resulted singly charged cluster ions detected via position-sensitive time-of-flight (PSTOF) mass spectrometry,[20] a technique which maps the longitudinal spatial distribution of the molecular beam onto the time domain. The spatial deflections or broadening of each cluster size was independently measured by quantitatively comparing the field-on versus field-off PSTOF peak profiles.

The calibration of the magnetic deflection magnitude was performed by the measurement of Ho atom deflection at T = 151 and 301 K. Figure 1a shows the expanded PSTOF peak of Ho atom in various magnitudes of magnetic-field gradients at T = 151 K. This spatial broadening is caused by the Zeeman splitting of the beam into $2J + 1$ equally spaced beamlets.[21] Since the ground state of the Ho atom is $^4I_{15/2}$, 16 beamlets corresponding to M_J = −15/2, ..., +13/2, +15/2 deflect according to their magnetic moment $\mu_z = -gM_J\mu_B$ where the Landé constant g = 1.2.[21] Therefore, the magnetic moment μ_z for the outmost beamlet is 9 μ_B. We note that μ_z differs from the magnetic

(16) Ivanova, A.; Baumgarten, M.; Karabunarliev, S.; Tyutyulkov, N. *Phys. Chem. Chem. Phys.* **2002**, *4*, 4795.
(17) Yasuike, T.; Yabushita, S. *J. Phys. Chem. A* **1999**, *103*, 4533.
(18) Miyajima, K.; Yabushita, S.; Nakajima, A.; Knickelbein, M. B.; Kaya, K. *J. Am. Chem. Soc.* **2004**, *126*, 13202.
(19) (a) Knickelbein, M. B. *J. Chem. Phys.* **2002**, *116*, 9703. (b) Knickelbein, M. B. **2002**, *116*, 9703. (c) Knickelbein, M. B. *Phys. Rev. B* **2005**, *71*, 184442.
(20) de Heer, W. A.; Milani, P. *Rev. Sci. Instrum.* **1991**, *62*, 670.
(21) Martin, W. C.; Zalubas, R.; Hagan, L. *National Standard Reference Data Series Number 60;* Gaithersburg, MD, 1978.

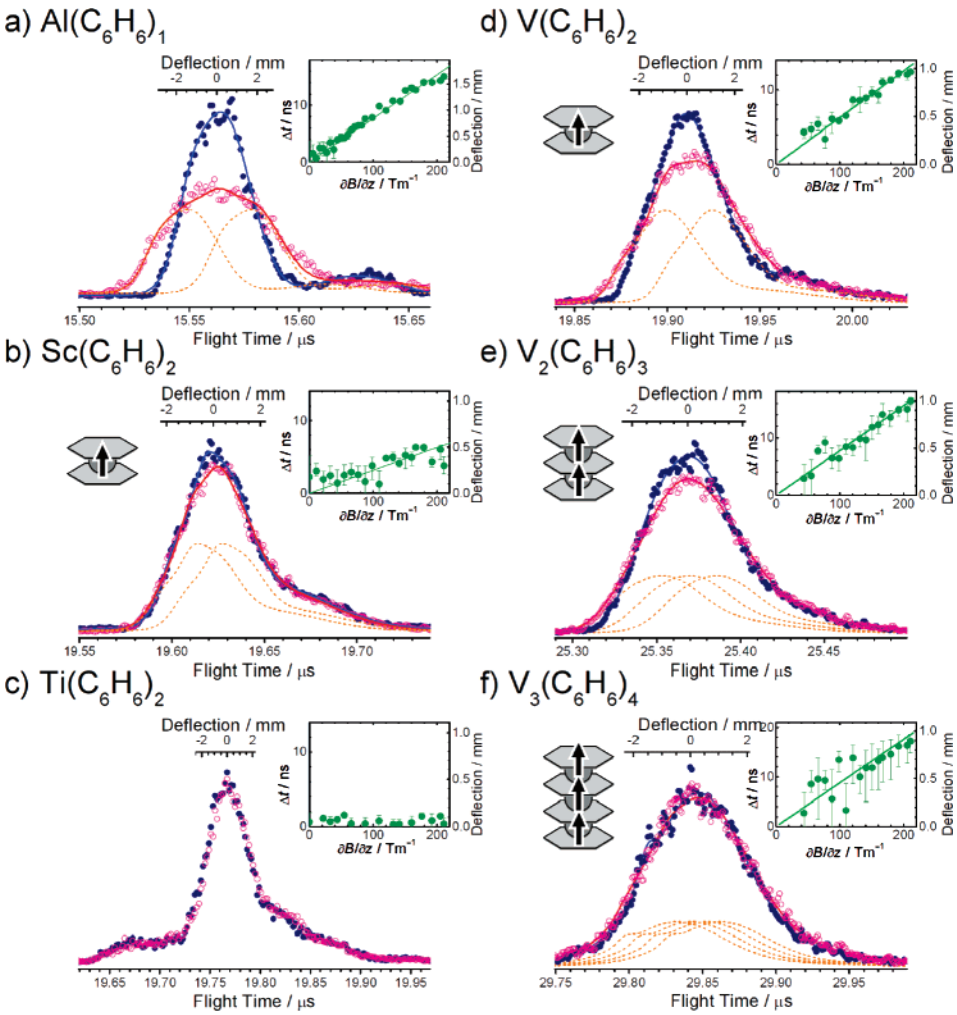

Figure 2. PSTOF spectra of $Al(C_6H_6)_1$, $Sc(C_6H_6)_2$, $Ti(C_6H_6)_2$, and $V_n(C_6H_6)_{n+1}$ ($n = 1-3$) clusters with and without magnetic-field gradient. (Filled blue circle, $\partial B/\partial z = 0$; open red circle, $\partial B/\partial z = 205$ Tm^{-1}) Temperatures of cluster source were $T = 152$, 152, 142, and 154 K for M = Al, V, Ti, and Sc, respectively. Solid lines indicate modeled PSTOF profiles for zero-field profile (blue) and simulated broadened profile (red). Beamlets are shown by dashed lines. Insets show the deflection magnitude of the outermost beamlet obtained by the beamlet model (see the text).

moment μ_{eff} often quoted in solid-state studies and is related to μ_z according to $\mu_{eff} = \{\mu_z\sqrt{J(J+1)}\}/J$. The spatial separation of the beamlets broadens the entire beam profile and hence the corresponding PSTOF peak profile. Since the deflection magnitude is very small in this example, each beamlet was not observed as separated Zeeman components because of the finite spatial width of the molecular beam and the limited spatial resolution of the PSTOF instrument. The asymmetric shape of the broadened Ho atom PSTOF peak at high field gradients is due to a variation of ion collection efficiency along the z direction. However, variation of the collection efficiency was negligibly small for the metal−benzene complexes in this study, because the complexes typically exhibit ten times smaller deflection compared to that of Ho atoms used in calibration studies. In this case, the PSTOF peak shapes of the sandwich clusters were analyzed without any corrections for the ion collection efficiency.

The spatial separation between the adjacent beamlets is extracted in a straightforward way by beam profile modeling, assuming that the field-broadened beam profile is composed of 2S + 1 equally spaced and equally intense beamlets. The inset plot of Figure 1a shows that the deflection magnitude increases lineally to the magnetic-field gradient ($\partial B/\partial z$). The slope of this plot gives the instrumental constant. Since the lowest electronic excited state $^6I_{17/2}$ lies above the ground state by 8.379×10^3 cm^{-1} (~1 eV), the contribution of excited states can be neglected in the temperature range of this study.

3. Results and Discussion

3.1. Mass Spectra and Calibration of the Magnetic Deflection of Al and Al(C$_6$H$_6$). Al−benzene clusters were produced by laser vaporization as described above. The only cluster produced in sufficient quantity for study using 193 nm photoionization was $Al(C_6H_6)$. Figure 1b shows beamlet-resolved magnetic deflection of the Al atom itself. Symmetric broadening and splitting of PSTOF profiles were observed as expected for a free-spin system.[20] This deflection behavior exhibited by the Al atom can be explained mainly by the two Zeeman sublevels ($M_S = \pm^1/_2$) of the ground state of $^2P_{1/2}$ ($g = {}^2/_3$) with minor contribution of an electric excited state Al($^2P_{3/2}$) ($g = {}^4/_3$). Since this $^2P_{3/2}$ electronic excited-state of Al lies 112.061 cm^{-1} (=0.013893 eV) above the ground state of Al($^2P_{1/2}$),[22] the population ratio of excited and ground states is estimated to be 4:6 at $T = 152$ K, assuming thermal equilibrium. The contribution of the excited states actually causes the observed peak broadening to be larger than that expected if only the $^2P_{1/2}$ ground state of Al is considered. The small bump at the low magnetic gradient in Figure 1b indicates this effect, which becomes even more prominent at room temperature. However,

(22) Martin, W. C.; Zalubas, R. *J. Phys. Chem. Ref. Data* **1979**, *8*, 817.

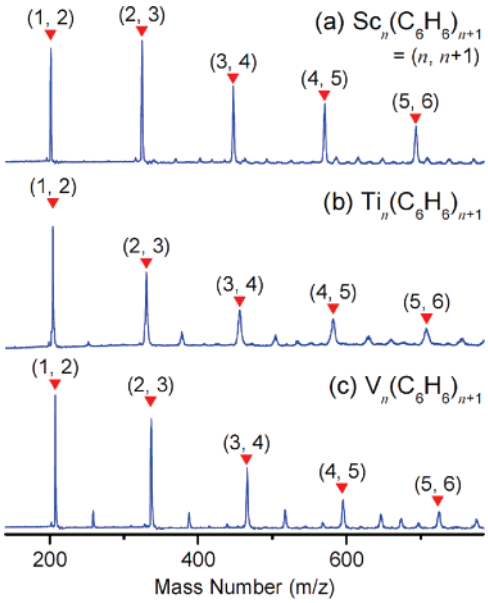

Figure 3. Mass spectra of $M_n(C_6H_6)_m$ (M = Sc, Ti and V) clusters. Temperatures of cluster source were T = 152, 142, and 154 K for M = V, Ti, and Sc, respectively.

the contribution of the excited-state is negligible in the high-magnetic gradient case, because beamlets of exited state deflect more and lose their shape faster. From analysis of the portions of the PSTOF beam profile attributable only to the ground state Al atoms, we find a magnetic moment for Al beamlets of $M_S = \pm^1/_2$ was determined as 0.32 ± 0.01 μ_B at T = 152 K, in agreement with the theoretical value ($\mu_z = \pm^1/_3$) within experimental uncertainty. This result demonstrates the general validity of the calibration method. For some studies, the Ho atom was used as a calibration standard in a similar way.

Figure 2a shows the expanded PSTOF spectrum for the Al-(C_6H_6) complex. Inspection of the mass spectrum shows that the Al(C_6H_6) complex was generated and photoionized without the occurrence of dehydrogenation. From the reported dissociation energy values for $Al^+(C_6H_6)$ and Al(C_6H_6), and estimated ionization energy for Al(C_6H_6) of around 5.0 eV,[23] we conclude that a single photon from the ArF excimer laser (6.42 eV) is sufficient to ionize the cluster without dissociation. We note that the Al$(C_6H_6)_2$ cluster was not produced in the same high abundances as the transition-metal benzene sandwich clusters. For the Al(C_6H_6) cluster (m/z = 105), there exists one unpaired electron coming from the Al 3p orbital,[24] and so its ground state is assumed to be doublet.[25] Accordingly, the analysis of PSTOF profile was performed assuming that it is composed of two deflected, but unresolved beamlets. This analysis revealed a magnetic moment of 0.70 ± 0.07 and 0.63 ± 0.05 μ_B at T = 54 and 152 K, respectively. The details of the spin-relaxation mechanism causing the experimentally determined values to be smaller than the ideal spin-only value, 1 μ_B, will be discussed in section 3.3.

3.2. Magnetic Deflection of Transition Metal−Benzene Clusters. Figure 3 shows typical photoionization mass spectra of transition metal−benzene clusters, $M_n(C_6H_6)_m$ (M = Sc, Ti and V), obtained with photoionization at 193 nm. In each mass spectrum, the peaks corresponding to sandwich clusters of (n, m) = (n, n + 1) appear prominently. This is a common feature for clusters composed of early transition metals and benzene molecules.[12,26] Small mass peaks between the *full* sandwich cluster (n, n + 1) peaks are readily assigned to the *open* sandwich clusters of (n, n) and (n + 1, n) in which excess metal atoms stick onto the terminal benzene(s).[27] Compared to previous studies in which the source was operated at room temperature,[26,28] we find that larger sizes of $Sc_n(C_6H_6)_{n+1}$ and $Ti_n(C_6H_6)_{n+1}$ (n = 3−5) are more abundant at lower source temperatures.

Figure 2 panels b−f show a detailed view of the PSTOF mass peaks corresponding to $Sc(C_6H_6)_2$, $Ti(C_6H_6)_2$, and $V_n(C_6H_6)_{n+1}$ (n = 1−3) with and without the magnetic field applied. Peak broadening was found for $Sc_n(C_6H_6)_{n+1}$ (n = 1, 2) and $V_n(C_6H_6)_{n+1}$ (n = 1−3) (the PSTOF peak of $Sc_2(C_6H_6)_3$ is not shown in the figure.) Qualitatively, this result indicates that the corresponding clusters have nonzero magnetic moments arising from unpaired spins and thus Zeeman splitting of the energy level into 2S + 1 equally spaced sublevels. In the beamlet analysis model used here, the broadened peak profile is expressed by the superposition of deflected zero-field peak profiles, with the degree of broadening determined by modeling the separation of the adjacent beamlets. For $M(C_6H_6)_2$ (M = Sc and V) clusters, their spin states are known to be spin doublets with Landé constant g = 2.[29−31] Using high-resolution photoelectron spectroscopy, Sohnlein et al. recently confirmed that the ground state of $Sc(C_6H_6)_2$ is doublet.[32] Lyon et al. have also found a double ground state for $Sc(C_6H_6)_2$ via a combined IR spectroscopic and DFT study.[29e] As shown in the insets of Figure 2, both $Sc(C_6H_6)_2$ and $V(C_6H_6)_2$ display broadening that increases linearly with magnetic-field gradient. From the slope of the broadening versus gradient plot, the magnetic moments μ_z for $Sc(C_6H_6)_2$ were evaluated to be 0.4 ± 0.1 μ_B at both T = 152 and 291 K. In a similar way, the magnetic moments μ_z for $V(C_6H_6)_2$ were evaluated to be 0.7 ± 0.1 and 0.7 ± 0.2 μ_B, respectively, at T = 154 and 296 K.

For the larger $Sc_n(C_6H_6)_{n+1}$ and $V_n(C_6H_6)_{n+1}$ sandwich clusters, analysis was carried out in a similar fashion, assuming that they adopt high-spin states with $S = {}^n/_2$ for each size n. For heavier species, it becomes difficult to distinguish whether they have nonzero magnetic moments or not, as both the deflection magnitude and the cluster abundance (and thus signal-to-noise ratios) become small. Moreover, the deflection magnitude becomes smaller at higher cluster source temperatures due to shorter transit time through the inhomogeneous magnet.

(23) (a) van Heijnsbergen, D.; Jaeger, T. D.; von Helden, G.; Meijer, G.; Duncan, M. A. *Chem. Phys. Lett.* **2002**, *364*, 345. (b) Mitchell, S. A.; Simard, B.; Rayner, D. M.; Hackett, P. A. *J. Phys. Chem.* **1988**, *92*, 1655.
(24) Howard, J. A.; Joly, H. A.; Mile, B. *J. Am. Chem. Soc.* **1989**, *111*, 8094.
(25) (a) Silva, S. J.; Head, J. D. *J. Am. Chem. Soc.* **1992**, *114*, 6479. (b) McKee, M. L. *J. Phys. Chem.* **1991**, *95*, 7247.
(26) Kurikawa, T.; Takeda, H.; Hirano, M.; Judai, K.; Arita, T.; Nagao, S.; Nakajima, A.; Kaya, K. *Organometallics* **1999**, *18*, 1430.
(27) (a) Miyajima, K.; Knickelbein, M. B.; Nakajima, A. *Eur. Phys. J. D* **2005**, *34*, 177. (b) Miyajima, K.; Knickelbein, M. B.; Nakajima *Polyhedron* **2005**, *24*, 2341.
(28) Yasuike, T.; Nakajima, A.; Yabushita, S.; Kaya, K. *J. Phys. Chem. A* **1997**, *101*, 5360.
(29) (a) McCamley, A.; Perutz, R. N. *J. Phys. Chem.* **1991**, *95*, 2738. (b) Andrews, M. P.; Mattar, S. M.; Ozin, G. A. *J. Phys. Chem.* **1986**, *90*, 744. (c) Andrews, M. P.; Mattar, S. M.; Ozin, G. A. *J. Phys. Chem.* **1986**, *90*, 1037. (d) Anderson, S. E., Jr.; Drago, R. S. *J. Am. Chem. Soc.* **1970**, *92*, 4244. (e) Lyon, J. T.; Andrews, L. *J. Phys. Chem. A* **2005**, *109*, 431.
(30) Kandalam, A. K.; Rao, B. K.; Jena, P.; Pandey, R. *J. Chem. Phys.* **2004**, *120*, 10414.
(31) Pandey, R.; Rao, B. K.; Jena, P.; Blanco, M. A. *J. Am. Chem. Soc.* **2001**, *123*, 3799.
(32) Sohnlein, B. R.; Li, S.; Yang, D.-S. *J. Chem. Phys.* **2005**, *123*, 214306.

Table 1. Magnetic Moments μ_Z/μ_B for $Sc_n(C_6H_6)_{n+1}$, $V_n(C_6H_6)_{n+1}$, and $Al(C_6H_6)_1$ Clusters[a]

	$\mu_{z\ 152\ K}/\mu_B$	$\mu_{z\ 291\ K}/\mu_B$
$Sc(C_6H_6)_2$	0.4 ± 0.1	0.4 ± 0.1
$Sc_2(C_6H_6)_3$	0.5 ± 0.2	$(0.7^{+0.5}_{-0.6})$
$Sc_3(C_6H_6)_4$	$(1.0^{+0.5}_{-0.4})$	
	$\mu_{z\ 154\ K}/\mu_B$	$\mu_{z\ 296\ K}/\mu_B$
$V(C_6H_6)_2$	0.7 ± 0.1	0.7 ± 0.2
$V_2(C_6H_6)_3$	$1.2^{+0.1}_{-0.2}$	$1.2^{+0.2}_{-0.3}$
$V_3(C_6H_6)_4$	$1.5^{+0.2}_{-0.4}$	$1.9^{+0.5}_{-1.1}$
$V_4(C_6H_6)_5$	$1.9^{+1.0}_{-0.9}$	
$V_5(C_6H_6)_6$	(2.6 ± 1.4)	
	$\mu_{z\ 152\ K}/\mu_B$	$\mu_{z\ 304\ K}/\mu_B$
$Al(C_6H_6)_1$	0.63 ± 0.05	0.7 ± 0.1

[a] μ_Z values are for the outmost beamlets corresponding to the maximum *M*s.

The deflection magnitude of $Sc_2(C_6H_6)_3$ at $T = 152$ K is, for example, close to the detection limit of our apparatus. Although it is difficult to conclude that the spin state of $Sc_2(C_6H_6)_3$ is triplet or a mixture of triplet and singlet, we conclude that the magnetic moment of $Sc_2(C_6H_6)_3$ to be nonzero, with an effective value of $0.5 \pm 0.2\ \mu_B$ at $T = 152$ K.

The magnetic deflections measured for $V_2(C_6H_6)_3$ and $V_3(C_6H_6)_4$ clusters increase linearly with *n*; their magnetic moments were determined to be $1.2^{+0.1}_{-0.2}$ and $1.5^{+0.2}_{-0.4}\ \mu_B$ at $T = 154$ K, respectively. Taking $V_3(C_6H_6)_4$ as an example, we have checked the possibility of coexisting spin states having multiplicity smaller than $S = {}^n/_2$ for each size *n*. When we used two beamlets (doublet; $S = {}^1/_2$) instead of four beamlets (quartet; $S = {}^3/_2$) for $V_3(C_6H_6)_4$, the magnetic moment obtained was $1.1^{+0.2}_{-0.4}\ \mu_B$, which is larger than the expected value of the spin-only ($1.0\ \mu_B$) for a state with $S = {}^1/_2$. Since spin relaxations were observed for $V(C_6H_6)_2$ and $V_2(C_6H_6)_3$ in common, some spin relaxation can be expected to occur for $V_3(V_6H_6)_4$ as well. This result shows that $V_3(V_6H_6)_4$ takes a high spin state with $S = {}^3/_2$, although we cannot rule out the possibility of the coexistence of low- and high-spin states. Albeit with fairly large experimental uncertainties, $V_4(C_6H_6)_5$ and $V_5(C_6H_6)_6$ clusters also have nonzero magnetic moments. As shown in Table 1 and Figure 4, the magnetic moments μ_z of $V_n(C_6H_6)_{n+1}$ increase monotonically with cluster size *n*.

As shown in Figure 4, a monotonic increase of the magnetic moment is apparent for clusters generated at both $T = 154$ and 296 K. At lower temperature below 100 K, however, the magnetic moments were considerably lower than the values obtained at 154 K.[27a] The suppression of size-dependence of the magnetic moments implies that the fragmentation involving loss of benzene occurs as a result of photoionization: $V_n(C_6H_6)_{n+1+p} \rightarrow V_n(C_6H_6)_{n+1} + pC_6H_6$, because benzene-rich clusters ($m > n + 1$) were observed to be abundant at the colder source temperatures. For $T = 154$ and 296 K, both of the plots exhibit the same trend within experimental uncertainty, indicating that the spin alignment seems invariant with temperature in this range of *T* investigated in this study. The monotonic increase of the $V_n(C_6H_6)_{n+1}$ magnetic moments indicates that the spins of the nonbonding d_σ electrons on the V metal centers align ferromagnetically, giving rise to magnetic moments which scale linearly with the number of layers. It should be noted that the magnetic moments obtained in this work are smaller than the expected value of the spin-only ($g = 2$) case and of that determined in an EPR experiment ($g = 1.987$) for $V(C_6H_6)_2$.[29,33] To examine the possible effects of dissociative ionization on the product distribution, we performed the magnetic deflection experiment ($T = 151$ K) under identical conditions except using a low-fluence KrF excimer laser ($\lambda = 248$ nm; $h\nu = 5.00$ eV) for photoionization. The broadening of the same magnitude was observed for $V_n(C_6H_6)_{n+1}$ $n = 2-4$, implying that fragmentation of large clusters into smaller clusters accompanying photoionization is not responsible for the reduced magnetic moments. Rather, we believe that spin-rotation interactions are responsible for these effects; for measurements carried out in the gas phase, the rotational degrees of freedom can couple to the spin degree of freedom. This mechanism and its effects on the measured magnetic moments will be discussed in section 3.3.

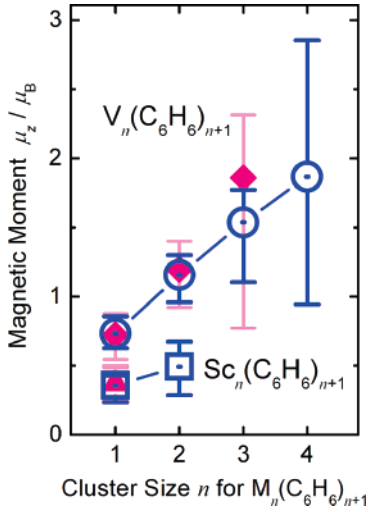

Figure 4. Magnetic moments μ_z for $Sc_n(C_6H_6)_{n+1}$ and $V_n(C_6H_6)_{n+1}$ clusters obtained by the beamlet model. Open circles/squares indicate the magnetic moments determined at ~150 K, whereas filled diamonds indicate the magnetic moments at room temperature.

In contrast to magnetically active $M(C_6H_6)_2$ (M = Sc and V) clusters, the magnetic moment for the $Ti(C_6H_6)_2$ cluster was determined to be near zero: $0.17^{+0.12}_{-0.13}\ \mu_B$ (assuming $2S + 1 = 3$). As shown in Figure 2c, no field-induced beam broadening was detected within experimental uncertainty. This result is in accord with the results of a photoelectron study in which it was determined that the electronic configuration of ground state $Ti(C_6H_6)_2$ was $^1A_1$.[33] Although we cannot rule out the presence of small contributions to the deflection profiles that may arise from electronically excited states having higher spin multiplicity, it seems reasonable to conclude that $Ti(C_6H_6)_2$ clusters can be regarded as nonmagnetic singlet species. However, $Ti_2(C_6H_6)_3$ and $Ti_3(C_6H_6)_4$ clusters were deflected slightly in the gradient magnetic field. As we will explain in section 3.4, DFT calculations have predicted a quintet ($2S + 1 = 5$) ground state for $n = 2$ and 3. Moreover, Kua et al. recently reported DFT calculation studies on the neutral, multiple-decker $Ti_n(C_6H_6)_m$ sandwich clusters,[34] and found quintet spin states for the ground states of $n = 2-4$ and a singlet ground state for $n = 1$. Assuming that the spin states of $Ti_2(C_6H_6)_3$ and $Ti_3(C_6H_6)_4$ are quintets as predicted theoretically, beamlet analyses were performed using five beamlets. This analysis showed that their magnetic moments

(33) Geoffrey, F.; Cloke, N.; Dix, A. N.; Green, J. C.; Perutz, R. N.; Seddon, E. A. *Organometallics* **1983**, *2*, 1150.
(34) Kua, J.; Tomlin, K. M. *J. Phys. Chem. A* **2006**, *110*, 11988.

were $1.0^{+0.5}_{-0.4}$ and $1.9^{+1.0}_{-1.4}$ μ_B at $T = 154$ K, respectively. Although these values are smaller than the expected spin-only value (4 μ_B), it is certainly possible that $Ti_2(C_6H_6)_3$ and $Ti_3(C_6H_6)_4$ might be produced as a quintet state together with states having lower spin multiplicity. Independently, another DFT calculation study by Xiang et al. suggested that the ground state for $Ti(C_6H_6)_2$ is again a singlet in contrast to an antiferromagnetic state for $[Ti(C_6H_6)]_\infty$ polymer, although the latter is more stable than the corresponding ferromagnetic state by only 0.006 eV.[35] Since the effects of terminal benzene molecules are exaggerated in these short 1D chains, the spin couplings in these shorter clusters can be different from those of the infinite 1D polymer.

3.3. Reduced Magnetic Deflection. In the case of the clusters considered in this study, the shapes and symmetries of deflected beam profiles are consistent with the free-spin (beamlet) model as shown in Figure 2, rather than with the locked-moment (the adiabatic spin rotor) or superparamagnetic behavior often displayed by other types of molecules and clusters.[36,37] However, as shown in the preceding section, the magnetic moments obtained in this work are smaller than the expected value of the ideal spin-only case. This is likely the result of coupling between rotational and spin degrees of freedom, a situation which leads to reduced effective moments[18,38−41] as a result of avoided crossings among the Zeeman sublevels.[42−44]

Although both $Sc(C_6H_6)_2$ and $V(C_6H_6)_2$ (each having one unpaired electron) are expected to display the same deflection behavior, the observed deflection magnitude displayed by $Sc(C_6H_6)_2$ is about half that of $V(C_6H_6)_2$; a similar tendency is observed for $Sc_2(C_6H_6)_3$ and $V_2(C_6H_6)_3$ clusters. It is noteworthy that the experimental conditions (He/benzene vapor gas mixture flow, vaporization laser power, cluster source temperature) are kept substantially the same for different metals so that any differences due to the variations in cluster beam conditions is negligible. Since both sandwich clusters have similar geometric structures, it follows that differences in the extent of magnetic moments-reduction reflect differences in the electron spin relaxation rates within the magnetic field.

In general, the relaxation rates of clusters will depend on their density-of-states, spin−orbit coupling, spin−rotation coupling, magnetic field strength, and their internal temperature.[38,44] The most striking difference in the electronic structures of $Sc(C_6H_6)_2$ and $V(C_6H_6)_2$ is the bonding character of the orbitals which accommodate the unpaired spin and the orbital angular momenta of the electrons in these orbitals. An unpaired spin in the $V_n(C_6H_6)_{n+1}$ sandwich cluster is accommodated in the nonbonding $d_\sigma(a_1)$ orbital on a V atom, while that of $Sc_n(C_6H_6)_{n+1}$ sandwich is accommodated in the bonding $d_\delta(e_2)$ orbital. The nonbonding character of the $d_\sigma(a_1)$ orbital reflects minimal overlap between metal d_{z^2} and ligand orbital, since the d_{z^2} orbital is oriented toward the center of the benzene molecular orbitals. The e_2 orbital, however, spreads over both the metal and the ligand.

In addition to the external magnetic field, there exist intracluster magnetic fields originating from the electron spin(s) and orbital angular momenta, and (to a lesser extent) from the rotational angular momenta of the molecular frame. Thus, the electron spin is essentially quantized in the direction of the external magnetic field, however, its direction is weakly related to the molecular frame through spin−orbit interaction, $\lambda\vec{l}\cdot\vec{s}$, and a much weaker spin−rotation interaction. In this way, the spin relaxation takes place because of the perturbations of spin−orbit and spin−rotation couplings. It can be expected that the electron spin in the d_σ orbital is only weakly affected by the direction of the cluster, since the spin−orbit coupling of this σ orbital is zero, so that only spin−rotation coupling becomes important. Moreover, this d_σ orbital is less affected by the molecular vibration because of its nonbonding character. On the other hand, a pair of degenerate d_δ orbitals have an orbital angular momentum of $\pm 2\hbar$ so that an electron spin is affected by the direction of the cluster, through the spin−orbit interaction. Furthermore these bonding orbitals would have stronger interactions with metal−ligand vibration. Therefore if the unpaired spin is accommodated in the e_2 orbital having nonzero angular momentum, it can be expected that faster intracluster spin relaxation shall occur. Thus, the different orbital angular momenta and bonding characteristics of open-shell orbitals qualitatively explain the different spin relaxation rates. Indeed, Amirav and Navon's systematic study on the organometallic complexes suggested that one of the reasons for the extremely fast spin relaxation observed for cobaltocene, $Co(C_5H_5)_2$ (whose ground state is $^2E_1$ ($a_1^2e_2^4e_1^1$)(ref 45)) is the significant contribution of the orbital angular momentum.[38] According to their results, intramolecular spin relaxation is intrinsic for sandwich complexes. They also proposed that the complexity and flexibility of those organometallic molecules are other contributing factors for the fast relaxation observed.

To estimate the effects of spin relaxation in the Stern−Gerlach deflection results, a simple random walk model for spin−flip was devised. Theoretical treatment of the effects of intramolecular electron-spin relaxation has been already reported by Gedanken et al.[46] With increasing flipping speed, the beamlet splitting pattern is effectively blurred together with a reduced beam broadening as a result. In the fast flipping limit, no field-induced broadening of the beam profile would be observed. In our implementation, the initial spatial distribution perpendicular to the beam direction was modeled as a Gaussian to reproduce the observed zero-field PSTOF peak profile. The spatial deviation from the beam was simulated by 100 trials involving spin−flips for 10^4 particles with various spin−flip probabilities and field gradients. Deflection magnitude was extracted from the simulated Stern−Gerlach beam profile by curve fitting, using the beamlet model used to analyze the experimental data. As shown in Figure 5, with increasing spin−flip rate the deflection magnitude quickly decreases and the separated beamlets in PSTOF profile are merged into a single peak. This behavior can be explained by the competition between the cluster's spin relaxation speed and transit speed through the magnet.

(35) Xiang, H.; Yang, J.; Hou, J. G.; Zhu, Q. *J. Am. Chem. Soc.* **2006**, *128*, 2310.
(36) (a) Bertsch, G. F.; Yabana, K. *Phys. Rev. A* **1994**, *49*, 1930. (b) Bertsch, G.; Onishi, N.; Yabana, K. *Surf. Rev. Lett.* **1996**, *3*, 435. (c) Bertsch, G.; Onishi, N.; Yabana, K. *Z. Phys. D* **1995**, *34*, 213.
(37) Knickelbein, M. B. *J. Chem. Phys.* **2006**, *125*, 044308.
(38) Amirav, A.; Navon, G. *Chem. Phys.* **1983**, *82*, 253.
(39) Malakhskii, A.; Gedanken, A. *J. Chem. Soc., Faraday Trans.* **1996**, *92*, 329.
(40) Jones, N. O.; Khanna, S. N.; Brunah, T.; Pederson, M. R. *Phys. Rev. B* **2004**, *70*, 045416.
(41) Knickelbein, M. B. *J. Chem. Phys.* **2004**, *121*, 5281.
(42) de Heer, W. A.; Milani, P.; Châtelain, A. *Z. Phys. D* **1991**, *19*, 241.
(43) Gedanken, A.; Kuebler, N. A.; Robbin, M. B.; Herrick, D. R. *J. Chem. Phys.* **1989**, *90*, 3981.
(44) Xu, X.; Yin, S.; Moro, R.; de Heer, W. A. *Phys. Rev. Lett.* **2005**, *95*, 237209.
(45) König, E.; Schnakig, R.; Kremer, S.; Kanellakopulos, B.; Klenze, R. *Chem. Phys.* **1978**, *27*, 331.
(46) Herrick, D. R.; Robin, M. B.; Gedanken, A. *Chem. Phys.* **1989**, *130*, 201.

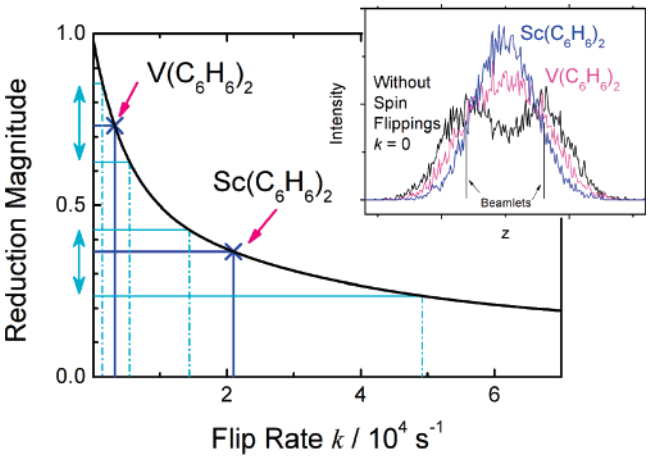

Figure 5. Simulated reduction magnitudes of magnetic deflection along with the spin−flip rate k for this work. Arrows and lines indicate the corresponding probabilities of vanadium and scandium sandwich clusters and their range of experimental uncertainties. Inset shows simulated PSTOF peak profiles at the same nonzero magnetic-field gradient but different spin−flip rates k, corresponding to $V(C_6H_6)_2$ and $Sc(C_6H_6)_2$. Intact beamlets ($S = \pm^1/_2$) at $k = 0$ are also shown as the reference.

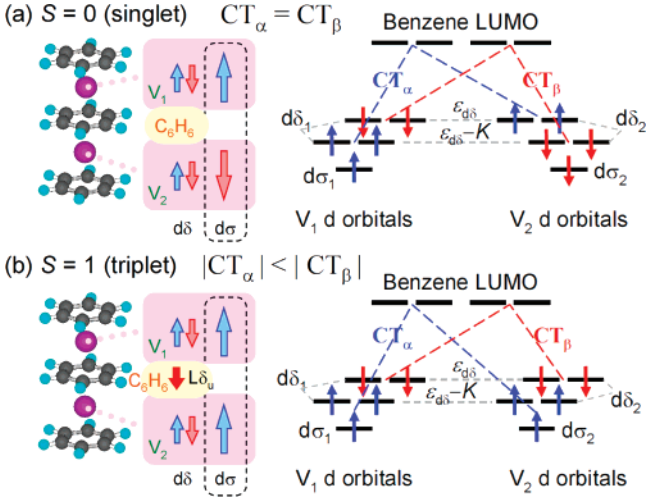

Figure 6. Schematic orbital diagrams in the charge transfer (CT) interactions in (a) singlet and (b) triplet cases for $V_2(C_6H_6)_3$. The orbital energy levels in the right side of this figure are those of fragment orbitals, $d_{\delta 1}$, $d_{\delta 2}$, and $L_{\delta u}$, from which delocalized molecular orbitals are constructed. The d_δ orbitals with the same spin with the singly occupied d_σ electron are stabilized by the intra-atomic exchange interaction (K).

In our setup, the transit velocities V are ∼1080 and ∼1370 ms^{-1} at $T = 154$ and 296 K, respectively, so that in both cases transit time is $\sim 2 \times 10^{-4}$ s which corresponds to the onset of the deflection reduction. The reductions of magnetic moment magnitudes of 73% and 36% at $T = 154$ (M = V) and 152 K (M = Sc) correspond to the spin−flip probabilities of 9×10^{-3} and 6×10^{-2}, which provide relaxation times of $t_{1/2} = 2 \times 10^{-4}$ and 3×10^{-5} s, and relaxation rate constants $k = 3 \times 10^3$ and 2×10^4 s^{-1}, respectively. This result well reproduces Figure 5 in ref 46, where the corresponding parameter λ = (life time)/(residence time) = τ/t = 0.8 and 0.1, respectively. Since the peak width of the undeflected TOF peak in our experiment is ∼4 times wider than in their simulation for $\sigma_0 = 0.30$, the characteristic trapezoidal shape at $\lambda = 0.8$ is completely buried in the present case. Under these conditions, the beamlet model is applicable to treat the reduced deflection pattern, in which they do not account for the distribution between each ideal beamlet. No significant differences from the $T = 150$ K result were found using the same analysis for room temperature. In the latter case, that is, $\lambda = 0.1$, the relaxed beamlet profile loses the splitting pattern completely. Strictly speaking, therefore, the use of the beamlet model to the high-temperature case becomes inappropriate for deducing the cluster's *intrinsic* magnetic moment accurately. Although a detailed and comprehensive understanding of spin relaxation mechanism is required to accurately determine a cluster's intrinsic magnetic moment in a gas-phase deflection experiment, the observation of nonzero magnetic moment species clearly provides vital pieces of information necessary for identifying molecular components which may be useful for assembling novel magnetic materials.

3.4. Mechanism of Ferromagnetic Spin Alignment. In this section, we describe the mechanisms responsible for ferromagnetic spin alignment deduced for $M_2(C_6H_6)_3$ (M = Sc, Ti, and V) using the results of all-electron DFT (B3LYP) calculations together with the 6-311G** basis functions. These calculations indicate that the electronic ground state of $Sc_2(C_6H_6)_3$ is a triplet, with the electronic configuration $....d\delta_u^4 d\delta_g^2 d\sigma_u^0 d\sigma_g^0$. Both unpaired electrons from the two Sc atoms are accommodated in the orthogonal and degenerate bonding $d\delta_g$ orbitals, and thus the triplet state is favored by exchange interaction, namely by Hund's rule. This result predicts the occurrence of ferromagnetic spin ordering within long chains of $Sc_n(C_6H_6)_{n+1}$, although it is possible that such an ordered chain may become unstable at finite temperature. Indeed Xiang et al. suggested that $[Sc(C_6H_6)]_\infty$ is paramagnetic.[35]

Kua et al. have recently reported that $Ti_2(C_6H_6)_3$ has a quintet ground state, on the basis of the calculation using DFT(B3LYP) and ECP methods.[34] Our theoretical calculations are consistent with their results and show that a quintet ground state with an electronic configuration of $....d\delta_u^4 d\delta_g^2 d\sigma_u^1 d\sigma_g^1$ is 4400 cm^{-1} more stable than the closed shell singlet state having the $....d\delta_u^4 d\delta_g^4 d\sigma_u^0 d\sigma_g^0$ valence configuration. The former configuration results in more intra-atomic exchange stabilization energy, while the latter has stronger Ti−benzene bonding stabilization as a result of greater charge transfer interactions. These results imply the relative importance of the intra-atomic exchange energy for these first row transition-metal compounds.

The mechanism of ferromagnetic interactions among the vanadium atoms in $V_n(C_6H_6)_{n+1}$ sandwich complexes has been theoretically investigated previously. In our early report, unrestricted Hatree−Fock (UHF) and DFT calculations for $V_2(C_6H_6)_3$ in the triplet state showed that the α spin density was large on each V atom and β spin density was localized on the central benzene molecule.[17] By contrast, in the singlet case spin density appeared only on the V atoms, and no spin density was found on the intervening benzene molecule. Plausible mechanisms for triplet stabilization was explained in terms of an intra-atomic exchange interaction within the metal d orbitals (between d_σ and d_δ) along with a partial charge transfer (CT) between the d_δ and the benzene LUMO, denoted as $L_{\delta u}$.[17] We now elaborate on this molecular orbital picture. The relevant orbitals for $V_2(C_6H_6)_3$ are shown in Figure 6, in which the different orbitals for different spins (DODS) picture is adopted. The d_δ orbitals with the same spin with the singly occupied d_σ electron are stabilized by the intra-atomic exchange interaction (K) compared to the opposite spin case. Because of the difference in the d_δ spin orbital levels, the magnitude of the CT interaction

depends on the spin manifold; in the case of $S = 0$ (singlet), the CT interaction by α spin electrons, CT_α, is equal to CT_β, while in the case of $S = 1$ (triplet), CT_β is greater than CT_α, inducing negative (β) spin density on the central benzene ring, strengthening the C_6H_6-V bond, and thus favoring the triplet state. Our theoretical results show that the triplet state is 75 cm^{-1} more stable than the corresponding singlet diradical state. It is noted that the negative spin densities on the individual C atoms on the central benzene molecule should be identical since the CT interactions in the doubly degenerate dδ manifold are identical for $V_2(C_6H_6)_3$.[34] Although the d_σ orbital is characterized as nonbonding, the strong intra-atomic exchange interaction between d_σ and d_δ leads to ferromagnetic ordering through the intervening benzene ligands in this one-dimensional system.

Other recent theoretical calculations are also consistent with the ferromagnetic ordering picture, showing that electron-spin multiplicities in the ground state are 2, 3, and 4 for $V_n(C_6H_6)_{n+1}$ ($n = 1-3$).[30,47] Moreover, many theoretical investigations of infinite metal benzene complex chains $[V(C_6H_6)]_\infty$ have been reported. Rahman et al. investigated the spin polarization of a $[V(C_6H_6)]_\infty$ wire,[48] and suggested that this system has a ferromagnetic order due to a double exchange mechanism, as originally suggested by Zener and discussed by Anderson and Hasegawa.[49] Kang et al.[50] and Maslyuk et al.[51] independently studied the origin of the ferromagnetic coupling of spins in $[V(C_6H_6)]_\infty$ by calculating its band structure using DFT and predicted that the ground state of the wire can be described as a 100% spin-polarized ferromagnet (half-metal). Recently, Xiang et al. investigated $[M_T(C_6H_6)]_\infty$ (M_T = Sc, Ti, V, Cr, and Mn) by DFT calculation and also found that $[V(C_6H_6)]_\infty$ is a quasi-half-metallic ferromagnet.[34] These calculation studies indicate sandwiched nonmagnetic organic molecules can be spin-polarized by coordination of metal atoms possessing unfilled d orbitals.

4. Conclusions

The magnetic moments of multidecker metal−benzene organometallic clusters containing Al, Sc, Ti, and V were determined by a Stern−Gerlach magnetic deflection experiment. A monotonic increase of the magnetic moment μ_z for $V_n(C_6H_6)_{n+1}$ ($n = 1-4$) and $Sc_n(C_6H_6)_{n+1}$ ($n = 1-2$) was found. Observed magnetic moments for the clusters are smaller than the ideal spin-only value. That magnetic moment reduction was dependent on the identity of the metal (and thus the electronic configuration in the complex) indicates that the different intramolecular spin relaxation rates observed for $Sc_n(C_6H_6)_{n+1}$ and $V_n(C_6H_6)_{n+1}$ arise from the orbital angular momenta and differing bonding character of the spin-containing orbitals. While $Ti(C_6H_6)_2$ was found to be nonmagnetic, $Ti_n(C_6H_6)_{n+1}$ ($n = 2$, 3) possesses nonzero magnetic moments. In the near future, the soft-landing of size-selected ferromagnetic metal−benzene clusters onto nanoscale designed surfaces[52] is expected to open exciting new possibilities for exploiting these complexes as nanomagnetic building blocks in applications such as recording media or spintronic devices.[5]

Acknowledgment. Use of the Center for Nanoscale Materials was supported by the U.S. Department of Energy, Office of Science, Office of Basic Energy Sciences, under contract DE-AC02-06CH11357. This work was partly supported by the 21st Century COE program "KEIO Life Conjugate Chemistry (KEIO-LCC)" from the Ministry of Education, Culture, Sports, Science, and Technology (MEXT), Japan, and by the Grant-in-Aid for Young Scientists (B) from MEXT. We acknowledge Ms. Ayami Goto for carrying out preliminary DFT calculations of $M_2(C_6H_6)_3$ (M = Sc, Ti, and V).

JA070137Q

(47) Wang, J.; Acioli, P. H.; Jellinek, J. *J. Am. Chem. Soc.* **2005**, *127*, 2812.
(48) Rahman, M. M.; Kasai, H.; Dy, E. S. *Jpn. J. Appl. Phys.* **2005**, *44*, 7954.
(49) Anderson, P. W.; Hasegawa, H. *Phys. Rev.* **1955**, *100*, 675.
(50) Kang, H. S. *J. Phys. Chem. A* **2005**, *109*, 9292.
(51) Maslyuk, V. V.; Bagrets, A.; Meded, V.; Arnold, A.; Evers, F.; Brandbyge, M.; Bredow, T.; Mertig, I. *Phys. Rev. Lett.* **2006**, *97*, 097201.
(52) (a) Mitsui, M.; Nagaoka, S.; Matsumoto, T.; Nakajima, A. *J. Phys. Chem. B* **2006**, *110*, 2968. (b) Nagaoka, S.; Matsumoto, T.; Okada, E.; Mitsui, M.; Nakajima, A. *J. Phys. Chem. B* **2006**, *110*, 16008. (c) Nagaoka, S.; Matsumoto, T.; Ikemoto, K.; Mitsui, M.; Nakajima, A. Submitted for publication.